# Habitat changes and changing predatory habits in North American fossil canids

B. Figueirido[1*], A. Martín-Serra[1], Z.J. Tseng[2], C. M. Janis[3]

[1] Departamento de Ecología y Geología, Facultad de Ciencias, Universidad de Málaga, Campus de Teatinos s/n, 29071-Málaga (Spain).

[2] Division of Paleontology, American Museum of Natural History, Central Park West at 79th Street, New York, NY (USA).

[3] Department of Ecology and Evolutionary Biology, Brown University, Providence, 29016, RI (USA).

* Author for correspondance:

Borja Figueirido

*Departamento de Ecología y Geología de la Facultad de Ciencias de la Universidad de Málaga, 29071-Málaga, Spain*

E- mail: Borja.figueirido@uma.es

Telephone: +34 952131856

The spread of open grassy habitats and the evolution of long-legged herbivorous mammals with high-crowned cheek teeth have been viewed as an example of coevolution. Previous studies indicated that specialized predatory techniques in carnivores did not correlate with the spread of open habitats in North America. Here, we analyze new data on elbow-joint shape for North American canids over the past ~37 million years and show that incipiently specialized species first appeared along with the initial spread of open habitats in the late Oligocene. Elbow-joint morphologies indicative of the behavior of modern pounce-pursuit predators emerged by the late Miocene coincident with a shift in plant communities from $C_3$ to $C_4$ grasses. Finally, pursuit canids first emerged during the Pleistocene. Our results indicate that climate change and its impact on vegetation and habitat structure can be critical for the emergence of ecological innovations and can alter the direction of lineage evolution.

## INTRODUCTION

The future effect of anthropogenic climate change on current biodiversity is a matter of significant concern[1-3]. However, although predictive models can give important clues to short-term biotic reactions[4-5], only the fossil record can provide empirical data on evolutionary responses during long periods of profound climatic and environmental change[6-9]. Here we demonstrate that the evolution of predatory behaviour in North American canids (e.g., foxes and wolves; family Canidae) has been influenced by climatic and environmental transformation over the later Cenozoic (the past ~37 million years [Ma]). During this time, Earth's climate underwent a profound transition in higher latitudes, from climates that were warmer and more humid than today to a later cooling which resulted in increasingly modern climatic regimes[10]. This climatic trend was also accompanied by a marked transition in vegetation structure indicative of increasingly open habitats over the more forested ones[11]. Plant silica microfossils (phytoliths) attest that open-habitat grasslands were well established in North America by the end of the Oligocene at ~27-23 Ma[12]. This trend towards habitat opening had a strong impact on mammalian palaeocommunities, as evidenced by changes in ungulate (hoofed mammals) craniodental morphology indicative of feeding on more abrasive forage (e.g., hypsodont [high-crowned] cheek teeth), and changes in limb morphology to the elongate limbs typical of present-day fast-running (cursorial) open habitat ungulates[8,13,14]. However, while large herbivores are the faunal components directly impacted by vegetational change, the effect of such changes on large carnivores has been less studied. Some previous studies suggest that carnivores with limb morphology indicative of fast running did not evolve until the Pliocene[13,15,16], and therefore ~20 Ma after the initial spread of open grassy habitats and the evolution of the long-legged ungulates.

Here we use the impressive and well-documented fossil record of North American canids[17-19] to test if their inferred locomotor/predatory behaviour was influenced by Cenozoic environmental change towards open habitats, as has been documented in the contemporaneous large herbivores[8,11,14]. We test for direct association between predatory behaviour and environmental events, rather than an "arms-race" hypothesis between predators and prey. We use statistical shape analysis on two-dimensional anatomical landmarks drawn from the anterior surface of the humeral distal epiphysis to analyse the shape of the elbow joint in extinct canids (Fig. 1a), ranging from the Oligocene (~37 Ma) to the end of the Pleistocene (~0.01Ma), in comparison with a large sample of modern carnivores of known predatory behaviour. We analyse the shape of the elbow joint because it is an established morphological indicator of locomotor/predatory behaviour in living carnivores[20-22], as it reflects the relative range of forearm motion (Fig. 1b). Whereas ambush predators need to retain supinatory ability (i.e., rotation of the manus to palm-upwards position) to grapple with prey, both pursuit (long-distance running[23]) and pounce-pursuit (short-distance sprinting[23]) carnivores have forelimbs with the manus more locked into a prone position, and limb movement more restricted to the parasagittal plane[21,22].

The study confirms that the elbow joints of canids became increasingly modified towards morphology indicative of fast-running predatory behaviour in correlation with the progressive spread of grasslands in the later Cenozoic. We specifically show that: (i) early Oligocene canids were all generalized ambushers; (ii) more cursorial borophagine canids incipiently specialized towards pounce-pursuit predation appeared along with the initial spread of open habitats in the late Oligocene; (iii) although a second incipient specialization towards pounce-pursuit predation appeared within early cursorial canine canids, morphologies of modern specialized pounce-pursuit predators appeared in the

102 late Miocene (~7 Ma), coincident with a shift in plant communities from $C_3$ to $C_4$
103 grasses[24]; and *(iv)* true pursuit and endurance canids only appeared with the colder and
104 more arid conditions of the Pleistocene (~ 2 Ma). Our results demonstrate that climate
105 change and its impact on vegetation and habitat structure can be critical for the
106 emergence of ecological innovations and can alter the direction of lineage evolution.

107

108 **RESULTS**

109 **Assessing the phylogenetic signal in elbow size and shape**

110 The permutation test performed to assess for the presence of phylogenetic structure in
111 the elbow joint (Fig. 1), using the phylogeny shown in Supplementary Fig. 1 gave
112 statistically significant results for both elbow size (Permutation test for phylogenectic
113 signal; *Tree length*: 3.766; *P*-value: <0.0001; 10,000 rounds) and shape (Permutation
114 test for phylogenectic signal; *Tree length*: 0.226; *P*-value: <0.0001; 10,000 rounds).
115 Furthermore, the multivariate regression of elbow shape on size was highly significant
116 (Permutation test; N = 59; *P*-value: 0.0002; 10,000 rounds) with a percentage of elbow
117 shape explained for by size differences of 15.09%, which indicates an effect of
118 interspecific allometry. However, the multivariate regression of both contrasted
119 variables after accounting for phylogenetic effects was not significant (Permutation test;
120 N = 58; *P*-value: 0.7564; 10,000 rounds), indicating an absence of evolutionary
121 allometry. Furthermore, the phylogenetic signal of the size-free shape residuals was also
122 significant (Permutation test for phylogenetic signal; *Tree length* = 0.2339; *P*<0.0001;
123 10,000 rounds). Therefore, the significant correlation of shape on size obtained above
124 was due to phylogenetic patterning, and thus size-correction of the data was not
125 necessary. For this reason, we employed the Procrustes coordinates (Proc) of elbow
126 shape in subsequent multivariate analyses.

The regressions performed between the independent contrasts and their standard deviation yielded a non-significant result for both elbow shape (Permutation test; N = 58; *P*-value = 0. 6804; 10,000 rounds) and centroid size (Permutation test; N = 58; *P*-value = 0.8721; 10,000 rounds), which indicates that our shape and size data and our assembled tree fit adequately[25] and demonstrates that the independent contrast analyses were correctly made.

**Predatory behaviour**

The Canonical Variates Analysis (CVA) performed from the Procrustes coordinates (Proc) of elbow shape using the extant sample (Table 1) yielded two canonical functions (Canonical axis I: $\lambda$ = 3.01, Variance (%) = 83.4; Canonical axis II: $\lambda$ = 0.659, Variance (%) = 16.6). As indicated by the permutation test, both axes allowed a significant separation between the three pairs of predatory groups using both, the pairwise Mahalanobis distances and the pairwise Procrustes distances among groups (Table 2; see also Supplementary Table 1). The first function (Fig. 2a) clearly distinguishes ambush predators from predators more specialized for running (i.e. pounce-pursuit and pursuit, both known as cursorial) according to one set of morphological traits (Fig. 2b). The second function, however, separates both specialized predatory groups: pounce-pursuit predators from pursuit ones (Fig. 2a), showing a distinction between these two specialized hunting techniques according to a set of morphological traits (Fig. 2c). The calculation of the scores for extinct canids (Table 3) on both canonical functions provided a classification of fossil species into one of the three predatory groups according to their proximity to group centroids of extant carnivoran hunting techniques (Supplementary Table 2). The inferred scores for the three subfamilies are plotted in Fig. 2d.

Furthermore, the result of the phylogenetic MANOVA of both canonical axes is significant for predatory behavior (Wilks = 0.19018, F = 15.517; Pphyl = 0.01598), which indicates that the difference between predatory groups in CVA is significant even after accounting for phylogenetic relationships.

**Elbow-shape ancestral states**

The reconstructed elbow shapes for the ancestors of the three subfamilies using the weighted squared-change parsimony algorithm[26] clearly resemble the unspecialized elbows of modern ambush predators (Fig. 3; Nodes 13, 18). However, while the basal hesperocyonines never evolved towards a more cursorial mode of hunting behaviour, the elbow morphologies of some derived borophagines were intermediate between those of living ambushers and the living pounce-pursuit canines, indicating some loss of supination in these forms (Fig. 2d; Fig. 3). Thus we conclude that the pounce-pursuit hunting technique evolved at least twice, independently within the Borophaginae and Caninae (Fig. 3). In contrast, the reconstructed elbow shape for the ancestral node of the subfamily Caninae excluding the most basal canine sampled (*Leptocyon vulpinus*), i.e., the ancestral state for the tribes Canini plus Vulpini (see Fig. 3), represents a step forward in locomotor specialization towards pounce-pursuit from the more basal borophagines to living canines (Fig 3; Node 35). Furthermore, a clear shift in elbow-joint shape occurred at the ancestral node of the tribe Canini (Fig 3; Node 37), representing the first appearance of elbow morphologies characteristic of fast-running canids over long distances.

**Body mass estimation**

The body masses of extant species (Supplementary Table 3) regressed on the log-transformed centroid size resulted in highly significant line of best fit ($r$ = 0.976; $F$=524.412; $P$<0.00001). The %PE was 18.28 % and the % SEE was 25.75%. The

predicted body mass values for extinct canids using the function generated from extant data are shown in Supplementary Table 4. Although, the first species that reached or exceeded the postulated threshold value in carnivore biology of 21.5 Kg for which species are able to take prey as large as, or larger than, themselves was the hesperocyonine *Osbornodon fricki* at ~15-18Ma, species exceeding this physiological threshold were not common until the appearance of the Aelurodontina and Borophagina subtribes of the family Borophaginae at ~15-7Ma. Finally, within the family Caninae, species reaching or exceeding the 21.5 Kg threshold were common at the beginning of the Pleistocene with the appearance of some species of the genus *Canis* at around 2Ma.

**Enamel specialization**

The results of the analysis on the enamel Hunter-Schreger Band (HSB) specialization in canids are shown in Supplementary Table 5. In summary, hesperocyonine canids exhibit little or no development of acute or zig-zag angles in their cheek dentitions. In contrast, the initial increase in degree of HSB specialization occurred around ~23-22 Ma in borophagine canids and in the large and specialized *Enhydrocyon crassidens*. By ~15 Ma, HSB scores of >0.4 were common among borophagines, and fully zig-zag enamel prism bands (with the maximum HSB score of 1) appeared around 12-10 Ma in borophagines such as *Aelurodon taxoides*. The broad range of HSB scores represented by borophagine species and late Miocene canine species are maintained by Pleistocene and extant canines after the extinction of borophagines by the end of the Pliocene.

## DISCUSSION

Both of the canonical axes distinguished the extant forms into the three predatory behavioural groups (Fig. 2a; Supplementary Table 1). Furthermore, changes in elbow-joint shape captured by each axis show the morphological adaptations for

different types of predatory behaviour: ambush predators retain the generalized mammalian condition of relatively wide joints with high supinatory abilities, enabling grappling with the prey; pursuit predators have narrow and "box-like" elbows with limbs locked into a more prone position; and the elbow-joint morphology of pounce-pursuit predators is somewhat intermediate, but with some unique features[22] (Fig. 2b,c). It should be noted that, to a certain extent, among cursorial predators, pounce-pursuit versus pursuit behaviour is related to body size (but see Ref. 22): smaller carnivores (>20 kg) are pounce-pursuit predators and larger ones are pursuers, but some large pounce-pursuit predators exist (e.g., dingoes and the striped and brown hyenas).

When both of the canonical functions are applied to fossil taxa they indicate a directional change in elbow-joint shape over the past ~ 37 Ma: from that reflective of wide joints among the basal hesperocyonines, through the intermediate-shaped joints of borophagines, to the more "box-like" elbows of the Recent more derived canines (Fig. 2d), reflecting increasingly restricted forearm rotation. However, as evidenced by the reconstructed elbow shapes for the ancestors of the three canid subfamilies using parsimony-based algorithms, the basal hunting mode in all three canid clades was the more generalized ambush condition (Fig. 3a,b).

A qualitative proxy for cursorial abilities in living and extinct canids that supports our CVA results is the degree of reduction of the entepicondylar foramen in the anterior distal epiphysis of the humerus (Fig. 1a) as the degree of foramen reduction parallels other changes in forelimb morphology for cursorial efficiency[27]. In fact, although all hesperocyonines have a well-developed foramen and borophagines plus the primitive canine *Leptocyon vulpinus* have an intermediately-developed foramen, other more specialized cursorial canines greatly reduce the foramen (Supplementary Fig. 2). This progressive reduction through the evolution of canids seems to be associated with a

progressive restriction in forearm supination –a direct consequence of acquiring cursorial specialization. However, the absence of this entepicondylar foramen in some highly derived species of the genus *Borophagus* (see Supplementary Fig. 2) supports the evidence that the ambush type of predation secondarily evolved in large and derived borophagine canids.

Tracing changes of elbow-joint shape through time indicates that until ~30 Ma only ambush canids were present (Fig. 4b, 30Ma). Given that closed habitats today harbour mainly ambush predators[23], this morphology accords with the predominant Oligocene habitats dominated by woodlands[12]. This is also evidenced by the analysis of canid enamel microstructure, as these taxa did not experience any increasing of HSB folding in their teeth (Fig. 4b, 30Ma), indicating that early borophagine or hesperocyonine canids were not adapted to feed on bone (from carcasses) or inadvertently ingesting significant amounts of grit[28], both being items that are facilitated by the expansion of open environments[29-32].

In fact, palaeosols and fossil phytolith assemblages indicate that open habitats dominated by grasses were not common in North America until the latest Oligocene[12]. Our results indicate that this time was coincident with the first appearance of pounce-pursuit canids also adapted to an abrassive diet based on the combined elbow shape and enamel microstructure data. The earliest species classified by the CVA as incipient pounce predators were the small borophagines *Cormocyon haydeni* (*ca.* 3.6 Kg; ~19-29 Ma), *Desmocyon thompsoni* (*ca.* 10.5 Kg; ~17.5-24 Ma) and *Phlaocyon leucosteus* (*ca.* 3.7 Kg; ~16-22 Ma), coincident with proposed timing for the spread of grasses (Fig. 2d, Fig. 3; Supplementary Table 2). Studies of carbon isotope composition of palaeosols attest that this initial spread of grasses was due to the expansion of $C_3$ grasses over trees and shrubs, resulting in $C_3$ dominated ecosystems[33,34].

Some of these taxa show an initial increase of HSB folding (Fig 4b, 30-16Ma), which indicates some consumption of abrasive and/or hard items (grit or bone) typical of more open habitats[28-32] by these late Oligocene-early Miocene taxa. The increasing HSB folding in the teeth of the derived hersperocyonine *Enhydrocyon crassidens* (*ca.* 18.3 Kg; ~19-29 Ma) indicates that this ambush predator also inhabited in woodlands-savannahs (Fig. 4b, 30-16Ma) as living lions do today. Therefore, our data suggest that canids with specialized hunting techniques and durophagous diets of more open environments first appeared in accord with the proposed timing for the spread of grasses indicated by phytolith data[12].

From the Middle Miocene Climatic Optimum[35] (~16 Ma; MMCO; Fig. 4a) to the Late Miocene (~10.8 Ma) the diversity of pounce-pursuit canids increased, mainly due to the diversification of the subfamily Caninae. Following the MMCO, open habitats also increased in association with declining temperatures and increasing aridity[10,35] –an environmental pattern also tracked by the significant increase in the HSB folding of teeth enamel in post-MMCO taxa (Fig. 4b, 16-10.8Ma).

During the Late Miocene and Early Pliocene, this climatic and environmental trend was accompanied by an increasing specialization towards more cursorial abilities and more durophagous habits in canids, indicating that these taxa inhabited more open environments. In fact, the first appearance of elbow morphologies indicative of a pounce-pursuit behaviour and a high degree of HSB folding within canines took place at this time (Fig. 2d; Fig. 3; Fig. 4b, 10.8-0.5Ma). The pounce-pursuit behaviour first appeared in canine canids with some small-sized forms such as *Leptocyon matthewi* (~12.6-9 Ma) or *Leptocyon vafer* (~14-9Ma) (Fig 4; Supplementary Table 4) and the reconstructed elbow shape for the ancestral state of the tribes Canini plus Vulpini within the subfamily Caninae indicates a clear shift in elbow morphology toward the behavior

276 of pounce-pursuit predators (Node 35; Fig. 3). However, elbow morphologies typical of
277 modern pounce-pursuit predators first appear with early precursors of modern foxes
278 (i.e., *Vulpes stenognathus*) and an ancestral genus of modern canines (i.e., *Eucyon*
279 *davisi*) at ~5-9 Ma[36], as these taxa are the first that occupy a central position (not a
280 peripheral position) in the morphospace of modern pounce-pursuit predators (Fig 4b,
281 10.8-0.5 Ma).

282 Therefore, our data suggest an association between environmental change and
283 predatory behaviour, as this time was coincident with a marked shift in the dominant
284 photosynthetic pathway of grasses[24] –from $C_3$ to $C_4$– in turn associated with the spread
285 of extremely open savannas or prairies (Fig. 4a). The carbon isotope composition of
286 palaeosols confirms that $C_4$ grasses were not expanded until the late Miocene or early
287 Pliocene in North America[33,34]. However, the large canids of the late Miocene,
288 borophagines such as *Epicyon* or *Borophagus*, do not show any trend towards the
289 morphology of a pursuit, as most probably, they secondarily reverted to more ambush-
290 like elbow morphology, reflecting greater specialization at a larger body sizes (Fig. 3).
291 The coexistence of these large ambush borophagines with the earliest pounce canines
292 suggests a diversity of habitats in North America at this time. In fact, palaeosol data
293 indicate that habitats composed by $C_3$ trees and shrubs over a carpet a $C_4$ grasses[33,34].

294 Finally, following the extinction of the subfamily Borophaginae, during the
295 Pleistocene, members of the subfamily Caninae evolved large body sizes, echoing the
296 trend seen in both of the extinct subfamilies to become larger and more carnivorous
297 over time[36,37]. This evolutionary size increase, initially seen in the specialized late
298 Miocene pounce-pursuit members of the Caninae, led to the emergence during the
299 Pleistocene of large-sized (~50 Kg; Fig. 4c; Supplementary Table 4) long-distance
300 pursuit predators, with the appearance in North America of the grey wolf *Canis lupus*

and the extinct dire wolf *Canis dirus* (Fig. 2d; Fig. 3; Fig. 4b, 10.8-0.5 Ma). This result was confirmed by the reconstruction of the ancestral state of the tribe Canini whose shape clearly resembles the elbows of long-distance pursuit predators (Fig. 3b). The appearance of pursuit predatory behaviour was also coincident with the appearance of a degree of HSB folding in canine canids comparable to the HSB folding of earlier borophagines (Fig. 4b, 10.8-0.5 Ma). This suggests that the later specialized pursuit predators were adapted to inhabit extremely open prairies dominated by $C_4$ grasses[33,34]. As indicated by carbon isotope composition of palaeosols, this time was coincident with levels of $C_4$ grasses biomass (>50%) like those in some regions of North America today (i.e., Great Plains)[33,34]. In fact, around the same time other possible pursuit predators[13], such as the cheetah-like felid *Miracinonyx* or the fast-running hyena *Chasmaporthetes*, immigrated to North America from Eurasia[16].

Our results indicate that mammalian herbivores were not the only groups strongly influenced by Cenozoic climatic change and its impact on vegetation and habitat structure. Predators change their predatory habits when herbivores change their foraging behaviour in association with habitat opening related to climatic change. The dramatic response to environmental transformation by late Cenozoic canids reported here demonstrate that long periods of profound climatic change are critical for the emergence of ecological innovations and could alter the direction of lineage evolution.

## METHODS

### Materials, Landmarks and Geometric Morphometrics

The elbow joint-shape in the 139 specimens (92 living specimens distributed among the families Felidae, Hyaenidae, Viverridae, Mustelidae and Canidae of the order Carnivora [Table 1] and 47 fossil specimens of the family Canidae including representatives of the

three subfamilies, Hesperocyoninae†, Borophaginae† and Caninae[17-19] [Table 3] was recovered by digitizing six *landmarks* in 2D on the anterior surface of the humerus distal epiphysis[20-22] from high resolution digital images (Fig. 1a). The digital images were taken with a tripod and following a standardized protocol for avoiding lens distortion and parallax.

We sampled those families of living carnivores with large representatives such as canids, felids and hyenids, because the inclusion of viverrids and mustelids do not add crucial information in terms of body size or predatory behaviour. However, we also sampled the wolverine because it is the largest mustelid (*Gulo gulo*), an ambush predator, and the large African (*Civettictis civetta*) and Indian (*Viverra zibetha*) civets.

The six landmarks were digitized into two-dimensional Cartesian coordinates ($x$,$y$) using TPSdig V. 211[38] (Supplementary Data 1) but we modelled the inter-landmark distances by means of an outline to obtain clearer shape transformation models in subsequent multivariate analysis. Additionally, we superimposed the two-dimensional outlines into a three-dimensional scanned surface of a jaguar, *Panthera onca* (139959, AMNH) specimen in order to obtain clear interpretations of the shape transformation recovered in the axes derived from different multivariate approaches. All the specimens digitized were aligned using Procrustes and projected onto the tangent space[39]. The size of the specimens was represented by their centroid size (Cs), which allows post-hoc assessment for allometric effects[40]. Centroid size is the square root of the sum of squared distances of each landmark from the centroid of the configuration[40]. The calculation of Procrustes Coordinates (Proc) and Cs were performed with MorphoJ[41].

We used the same six landmarks as Andersson[20], as they are established morphological indicators of forearm pronation and supination. However, whereas Andersson[20] analyzed solely the Euclidean distances among landmarks, we used an

approach based on Geometric Morphometrics. Our approach not only captures the relative distances among the landmarks but also the topological information contained within them.

**The influence of size and phylogeny in elbow-joint shape**

We assembled a phylogenetic consensus tree (Supplementary Fig. 1) following various published sources using Mesquite[42]. We incorporated branch lengths in our composite phylogeny in million years before present[43,44]. In the case of living species, branches were scaled according to node dates estimates based on Nyakatura and Bininda-Emonds[45]. In the case of extinct taxa, fossil occurrence dates were compiled from various sources based on species locality and age information (Table 2), and the branch lengths were estimated from the first and last appearance of taxa (Supplementary Fig. 1). We used this phylogenetic tree to assess phylogenetic patterning in our data.

As we are only interested in quantifying the presence of phylogenetic signal, instead of the strength of the phylogenetic signal, we used the permutation approach developed by Laurin[46], extended for multivariate analysis by Klingenberg and Gidaszewski[47], and applied to shape data by other authors (e.g., 48-54), to simulate the null hypothesis of complete absence of phylogenetic signal in elbow shape. The mean species shapes are randomly distributed as the tips of the phylogeny in 10,000 permutations, and for each permutation, the tree length was computed. If the resulting tree length computed for each permutation was greater than the one obtained with the original data, the null hypothesis of absence of phylogenetic structure was rejected. A P-value was used for assessing the presence of phylogenetic signal in shape[47].

A multivariate regression analysis[55] of shape (i.e., using Proc) on size (i.e., using Cs) was performed to test the influence of allometry. In addition, we applied

independent contrasts analysis[56] to take into account the phylogenetic relationships of the species under study. Following this, we regressed the contrast for shape (Proc) on the contrast for size (Cs) using MorphoJ[41]. The statistical significance of both multivariate regression analyses was tested with a permutation test against the null hypothesis of complete independence of shape on size[57].

We performed a multivariate regression analysis[55] of the Independent contrast of the Proc against the standard deviation of the standardized contrast (i.e., the square root of the corrected branch lengths) with MorphoJ[41], following Díaz-Uriarte and Garland[25]. The values of the standard deviations were obtained from the PDAP module for Mesquite[42,58]. The significance of this regression was evaluated with a permutation test against the null hypothesis of complete independence between the two variables. This test was specifically performed to explore the adequacy of: *(i*) the model used for tree topology; *(ii)* the branch lengths used; and *(iii)* the model of Brownian motion for our tip data[25].

**Inferring predatory behaviour in extinct canids**

To determine those elbow-joint shape features that best distinguish among the three present-day predatory modes (ambush; pounce-pursuit; and pursuit), we performed a CVA from the Proc of elbow shape in modern predators. We used CVA instead of Principal Components Analysis (PCA) as performed by Andersson[20] because to find those elbow shape features that best distinguish among these predatory groups of specimens, the use of CVA is more appropriate than PCA. In fact, while CVA is a classification method, PCA is an ordination one. In any case, it is worth mentioning that although Andersson[21] also used CVA, the analysis was performed to differentiate among the three subfamilies of canids instead to infer their predatory behavior.

We classified all of the living species into one of the three present day predation modes following previously published sources[23,59] as follows: *(i)* ambush predators stalk their prey and may pursue them over short distances, and the forelimbs may be used to grapple with large prey; *(ii)* pounce/pursuit predators usually hunt small prey using either a pounce or short chase, and rarely grapple with their prey; And *(iii)* pursuit predators usually chase their prey for a long distance (> 30 m), and may hunt cooperatively to bring down large prey, but do not grapple with their prey (Table 1). Therefore, we consider here the pounce-pursuit category of Van Valkenburgh[23] instead of only "cursorial" and "non-cursorial" predators as Andersson[20] differenced. However, these three hunting types are usually correlated with prey size: while ambushers can take prey of all sizes, pounce predators usually take small prey and pursuit predators usually take large prey. Both ambush and pursuit predation can be directly linked to forearm mobility and elbow function in the case of large prey, but a predator will not "pounce" on large prey nor "pursue" small prey. We consider the cheetah (*Acinonyx jubatus*), the only highly cursorial felid, to be a pursuit predator, even though this species still retains some ability to supinate as they often swat their prey (but they do not grasp it). The reason is because the cheetah is a solitary hunter but does not have the endurance of the canid and hyenid pursuit predators and it will bring down its prey with the swipe of a forelimb. However, the cheetah is a felid that is clearly more specialized towards running than others in its family, pursuing its prey for a distance of up to 200 m and it has been classified as a pursuit predator by other researchers[15,59].

As the predatory categories used here are dynamic and not static, our predatory grouping scheme established by Van Valkenburgh[23] represents an arbitrary division of a continuous range. Furthermore, many carnivorous taxa range over some predatory types (e.g., the cheetah), and so the assignment of a given species to a particular category is a

426 'best fit' designation rather than an exclusive one. In summary, our predatory categories
427 are thus a significant (albeit necessary) simplification of the complex range of predatory
428 behaviour.

429 The reliability of group separation was assessed by the pairwise Procrustes
430 distances and Mahalanobis distances among all possible pairs of groups using the
431 pooled within-group covariance matrix for all the groups jointly. A permutation test was
432 computed for the Mahalanobis and Procrustes distances of all pairwise comparisons.
433 The statistical significance of these pairwise differences was assessed with 10,000
434 permutations using MorphoJ[41]. Both canonical functions obtained from the living
435 sample in CVA were later applied to fossil taxa using their Proc of elbow shape.
436 However, although we will never be sure if the established predatory categories based
437 on living carnivores can be extrapolated to extinct species, this uncertainty is alleviated
438 if fossil forms have extant relatives. This is particularly the case of the family Canidae,
439 as extant forms phylogenetically bracket them, where the morphological correlates of
440 behaviour are known.

441 We used the direct method of leave-one out cross validation for assessing the
442 percentage of probability of living canids to belong for one of the three present-day
443 predation modes. The classification of fossil species into one of the three predatory
444 groups was inferred according to their proximity to group centroids of the three
445 predatory groups of extant carnivorans with SPSS v.19.

446 We did not use the stepwise discriminant analysis[60] because we have more cases
447 per group than predictor variables; 12 variables or six bi-dimensional landmarks
448 digitized in 35 pounce-pursuit predators, 30 ambush predators and 22 pursuit predators
449 (Table 1). Thus, there is no statistical reason to perform a stepwise approach instead of

450 the direct method because CVA only tends to over fit differences in those cases where
451 there are more variables than the number of cases within groups[61].
452 The morphospace depicted from the scores of the living specimens into both
453 canonical axes was imported into the graphing software SigmaPlot to create a contour
454 plot that was colour coded by predatory mode –extant ambushers in blue, extant
455 pounce-pursuit predators in green and extant pursuit predators in red. Colour
456 degradation within each predatory group was calibrated to the frequency of the
457 specimens within each predatory group. After we performed this contour plot from the
458 scores of the living taxa, we repeated the same graphs but now including the fossils
459 according to their predicted predatory category obtained in CVA. We recovered a RGB
460 colour code for each fossil specimen according to its position in the contour plot living-
461 morphospace.
462 To test whether carnivores with different predatory behaviour differed in shape
463 irrespective of phylogeny, we used the aov.phylo function in the R package 'geiger'[62]
464 using both canonical axes. We used Brownian motion as a model for evolutionary
465 change and ran 1000 simulations to create an empirical null distribution to compare
466 with our sample.
467 **Ancestral elbow shape reconstruction**
468 All taxa excluding canids were pruned from the phylogenetic tree shown in Fig.
469 S1 using Mesquite[42]. The ancestral states, or internal phylogenetic nodes, were
470 reconstructed by squared-change parsimony[26] weighted by branch lengths using
471 MorphoJ[39]. The main purpose to reconstruct ancestral states was to explore patterns of
472 elbow-joint shape evolution and by extension the evolution of predatory behaviour in
473 canids. Also, we would be able to assess the most probable basal hunting technique for

474 the three subfamilies and when the specialized traits of the elbow are acquired though
475 the evolution of canids.

476 **Body mass estimation in extinct taxa**

477 To explore if elbow shape changes experienced by the evolution of the family
478 could be in part explained by a previously reported trend towards size increase through
479 canid evolution[37], we explored the issue of whether the appearance of canids with
480 morphology indicative of more cursorial behaviour (pounce-pursuit or pursuit) is the
481 result of their body mass reaching or exceeding 21.5 Kg, which is a threshold value in
482 carnivore biology: only carnivores of this size or greater take prey as large as, or larger
483 than, themselves[63].

484 We estimated the body masses (BM) of fossil canids by means of a least-square
485 bivariate regression of log-transformed BM on Cs for the extant taxa (Log (BM) = a +
486 bLog[Cs]) using SPSS v.19. Although both body mass and elbow centroid size are
487 variables, each with its own errors and distributions under the control of the
488 investigator, we chose the least-square regression model (instead of a type II) because
489 our purpose here was to explore the body mass dependency of elbow centroid size. Note
490 that the main objective here was to obtain a model in which body mass can be predicted
491 from elbow centroid size. For these reason we assumed dependence between both
492 variables[64].

493 The body mass for each extant species was taken from recent studies on body
494 mass estimation in extinct taxa[64-66] and references therein. Their Cs were then computed
495 as the Cs average for all the specimens belonging to the same species. The accuracy of
496 the bivariate regression function was evaluated by means of the *F*-statistic and
497 Pearson's correlation coefficient (*r*). However, as the correlation coefficient can be high
498 even with high residuals[67], it is not a highly appropriate statistic to evaluate the

predictive power of a regression equation. Thus, to evaluate the predictive power of the function, we computed the percent prediction error (%PE) and the percent standard error of the estimate (%SEE)[67]. Once we had confirmed the significance of the Log-BM on Log-Cs regression equation and its predictive power, we predicted body mass values for the extinct canids.

**Enamel microstructure specialization in extinct canids**

The association between environmental change and canid predatory behaviour was investigated using the arrangement of the enamel prism bands –known as bands of Hunter-Schreger (HSB)– as a proxy. The reason is because carnivores that live in open environments consume more intrinsic (bones from carcasses) and extrinsic (grit) hard food items, which relates to heavily folded HSB[28, 51, 68-70]. Studies of carnivorans demonstrate a link between bone and carcass consumption and increased kleptoparasitism in open habitats because of increased carcass detectability[30-32]. Therefore, we utilize HSB analysis as proxy of habitat openness, in terms of increased enamel resistance to wear from ingested grit, as well as hard vertebrate tissue consumption associated with increased carcass availability in open environments.

To quantify the degree of specialization in the enamel prism bands arrangement (bands of Hunter-Schreger; HSB), we used a stereomicroscope at 5-40x magnification. We coded for each tooth in the dentition, the degree of HSB specialization in each of the three regions on the tooth crown (base, tip, and the mid-region), each occupying approximately one-third of total crown height. We quantified the degree of HSB specialization as follows: the less specialized undulating pattern, then the intermediate acute-angled undulating pattern, and followed by the most specialized zig-zag HSB pattern[70]. The final dataset included both newly collected data as well as published data in Tseng[69] (Supplementary Table 5).

The coded HSB pattern for each tooth was given as a score from 0 (for undulating pattern in all three regions of the tooth crown) to 1 (for zig-zag pattern in all three regions of the crown). We studied lower cheek dentitions (premolars and molars) of fossil canid species. However, we used the upper dentitions for those species without preserved dentaries. Furthermore, where both left and right dentitions were available, averages of scores were taken across the corresponding tooth and treated as a single entry in the data analysis. Because not all fossil specimens contained complete data for the premolar-molar sequence, 10% of the dataset represent composite HSB data from multiple specimens of the same species. The final HSB score for each specimen data point was calculated per tooth (total HSB score divided by number of teeth coded per specimen) to account for differences in completeness and tooth count of sampled species (Supplementary Table 5).

**REFERENCES**

1. Intergovernmental Panel on Climate Change (IPCC), Climate Change 2007 Synthesis Report (IPCC, Geneva, 2007).

2. Thomas, C. D.et al. Extinction risk from climate change. Nature 427, 145–148 (2004).

3. Sala, O. E. et al. Global Biodiversity Scenarios for the Year 2100. Science 287, 1770-1774 (2000).

4. Araújo, M. B. & Rahbek, C. How Does Climate Change Affect Biodiversity? Science 313, 1396-1397 (2006).

5. Araújo, M. B., Pearson, R.G., Thuiller, W. & Erhard, M. Validation of species-climate impact models under climate change. Glob. Change Biol. 11, 1504-1513 (2005).

549 6. Figueirido, B., Janis, C. M., Pérez-Claros, J. A., De Renzi, M. & Palmqvist, P.
550 Cenozoic climate change influences mammalian evolutionary dynamics. Proc. Nat.
551 Acad. Sci. USA 109, 722-727 (2012).
552 7. Eronen, J. T. et al. Distribution History and Climatic Controls of the Late Miocene
553 Pikermian Chronofauna. Proc. Natl. Acad. Sci. USA 106, 11867-11871 (2009).
554 8. Mihlbachler, C. M., Rivals, F., Solounias, N. & Semprebon, G. M. Dietary Change
555 and the evolution of horses in North America. Science 331, 1178 (2011).
556 9. Woodburne, M. O., Gunnell, G. F. & Stucky, R. K. Climate directly influences
557 Eocene mammal faunal dynamics in North America. Proc. Natl. Acad. Sci. USA 106,
558 13399-13403 (2009).
559 10. Eronen, J. T. et al. Neogene aridification of the Northern Hemisphere. Geology 40,
560 823-826 (2012).
561 11. Janis, C. M. Tertiary mammal evolution in the context of changing climates,
562 vegetation, and tectonic events. Annu. Rev. Ecol. Syst. 24, 467-500 (1993).
563 12. Strömberg, C. A. E. Decoupled taxonomic radiation and ecological expansion of
564 open-habitat grasses in the Cenozoic of North America. Proc. Natl Acad. Sci. USA 102,
565 11980-11984 (2005).
566 13. Janis, C. M. & Wilhelm, P. Were there mammalian pursuit predators in the tertiary?
567 Dances with wolf avatars. J. Mamm. Evol. 1, 103-125 (1993).
568 14. Janis, C. M., Damuth, J., Theodor, J. M. Miocene ungulates and terrestrial primary
569 productivity: Where have all the browsers gone? Proc. Natl Acad. Sci. USA 97, 7899-
570 7904 (2000).
571 15. Andersson, K. & Werdelin, L. The evolution of cursorial carnivores in the Tertiary:
572 implications of elbow–joint morphology. Proc. R. Soc. Lond. B 270, S163–S165
573 (2003).

574 16. Van Valkenburgh, B. Major patterns in the history of carnivorous mammals. Annu.
575 Rev. Earth Pl. Sc. 27, 463-493 (1999).
576 17. Wang, X. Phylogenetic systematics of the Hesperocyoninae (Carnivora: Canidae).
577 B. Am. Mus. Nat. Hist. 221, 1-207 (1994).
578 18. Wang, X., Tedford, R. H. & Taylor, B. E. Phylogenetic systematics of the
579 Borophaginae (Carnivora: Canidae). B. Am. Mus. Nat. Hist. 243, 1-391 (1999).
580 19. Tedford, R. H., Wang, X. & Taylor, B. E. Phylogenetic systematics of the North
581 American fossil Caninae (Carnivora: Canidae). B. Am. Mus. Nat. Hist. 325, 1-218
582 (2009).
583 20. Andersson, K. Elbow-joint morphology as a guide to forearm function and foraging
584 behaviour in mammalian carnivores. Zool. J. Linn. Soc-Lond. 142, 91-104 (2004).
585 21. Andersson, K. Were there pack-hunting canids in the Tertiary and how can we
586 know? Paleobiology 31, 56-72 (2005).
587 22. Figueirido, B. & Janis, C.M. The predatory behaviour of the thylacines: Tasmanian
588 tiger or marsupial Wolf? Biol. Letters 7, 937-939 (2011).
589 23. Van Valkenburgh, B. Locomotor diversity within past and present guilds of large
590 predatory mammals. Paleobiology 11, 406-428 (1985).
591 24. Edwards, E. J. et al. The origins of C4 grasslands: integrating evolutionary and
592 ecosystem science. Science 328, 587-591 (2010).
593 25. Díaz-Uriarte, R. & Garland, T. Effects of branch length errors on the performance of
594 phylogenetically independent contrasts. Syst. Biol. 47, 654-672 (1998).
595 26. Maddison, W. P. Squared-changed parsimony reconstruction of ancestral states for
596 continuous-valued characters on a phylogenetic tree. Syst. Zool. 40, 304-314 (1991).
597 27. Landry Jr, S. O. The function of the entepicondylar foramen in mammals. Am. Midl.
598 Nat. 100-112, (1958).

599 28. Tseng, Z. J. Connecting Hunter-Schreger Band microstructure to enamel microwear
600 features: New insights from durophagous carnivores. Acta Palaeontol. Pol. 57, 473-484
601 (2012).
602 29. Pfretzschner, H. U. Enamel microstructure in the phylogeny of the Equidae. J.
603 Vertebr. Paleontol. 13, 342-349 (1993).
604 30. Mills, M. G. L., Broomhall, L. S., & du Toit, J. T. Cheetah Acinonyx jubatus feeding
605 ecology in the Kruger National Park and a comparison across African savanna habitats:
606 is the cheetah only a successful hunter on open grassland plains? Wildlife Biol. 10, 177-
607 186 (2004).
608 31. Carbone, C., Cowlishaw, G., Isaac, N. J., & Rowcliffe, J. M. How far do animals
609 go? Determinants of day range in mammals. Am. Nat. 165, 290-297 (2005).
610 32. Gorini, L., Linnell, J. D., May, R., Panzacchi, M., Boitani, L., Odden, M., & Nilsen,
611 E. Habitat heterogeneity and mammalian predator–prey interactions. Mammal Rev. 42,
612 55-77 (2012).
613 33. Fox, D.L., & Koch, P.L. Tertiary history of C4 biomass in the Great Plains, USA.
614 Geology 31, 809-812 (2003).
615 34. Fox, D.L., & Koch, P.L. Carbon and Oxygen isotopic variability in Neogene
616 Paleosol carbonates: constraints on the evolution of the C4-grasslands of the Great
617 Plains, USA. Palaeogeogr. Palaeocl. Palaeoecol. 207, 305-329 (2004).
618 35. Zachos, J. C., Dickens,G. R. & Zeebe, R. E. An early Cenozoic perspective on
619 greenhouse warming and carbon-cycle dynamics. Nature 451, 279 (2008).
620 36. Wang, X., Tedford, R. H. & Antón, M. Dogs: their fossil relatives and evolutionary
621 history (Columbia Univ. Press, 2008).
622 37. Van Valkenburgh, B., Wang, X. & Damuth, J. Cope's Rule, Hypercarnivory, and
623 Extinction in North American Canids. Science 306, 101-104 (2004).

624 38. Rohlf, J. TpsDig, version 2.12. (Stony Brook, NY: Department of Ecology and
625 Evolution, State University of New York at Stony Brook, 2008).
626 39. Dryden, I. L. & Mardia, K. Statistical Analysis of Shape. (Wiley, Chichester, 1998).
627 40. Bookstein, F. 1998. Morphometric tools for landmark data. Geometry and biology.
628 (Cambridge Univ. Press, Cambridge, 1991).
629 41. Klingenberg, C.P. MorphoJ (Faculty of Life Sciences, University of Manchester,
630 Manchester, 2011). Available from: http://www.flywings.org.uk/MorphoJ page.htm.
631 42. Maddison, W. P. & Maddison, D. R. Mesquite: a modular system for evolutionary
632 analysis. Version 2.75. Available via http://mesquiteproject.org. (2011).
633 43. Polly, P. D. Paleontology and the comparative method: Ancestral node
634 reconstructions versus observed node values. Am. Nat. 157, 596-609 (2001).
635 44. Finarelli, J. A. & Flynn, J. J. Ancestral state reconstruction of body size in the
636 Caniformia (Carnivora, Mammalia): the effects of incorporating data from the fossil
637 record. Syst. Biol. 55, 301-313 (2006).
638 45. Nyakatura, K. & Bininda-Emonds, O. R. P. Updating the evolutionary history of
639 Carnivora (Mammalia): a new species-level supertree complete with divergence time
640 estimates .BMC Biol 10, 12 doi:10.1186/1741-7007-10-12 (2012).
641 46. Laurin. The evolution of body size, Cope's rule and the origin of amniotes. Syst.
642 Biol. 53, 594-622 (2004).
643 47. Klingenberg, C. P., & N. A. Gidaszewski. Testing and quantifying phylogenetic
644 signals and homoplasy in morphometric data. Syst. Biol. 59, 245–261 (2010).
645 48. Gidaszewski, N. A., M. Baylac, & C. P.Klingenberg. Evolution of sexual
646 dimorphism of wing shape in the Drosophila melanogaster subgroup. BMC Evol. Biol.,
647 9-110 (2009).
648 49. Figueirido, B., F. J. Serrano-Alarcón, G. J. Slater, & P. Palmqvist. Shape at the

649 cross-roads: homoplasy and history in the evolution of the carnivoran skull towards
650 herbivory. J. Evol. Biol. 23, 2579-2594 (2010).
651 50. Klingenberg, C. P., S. Dutke, S. Whelan, and M. Kim. Developmental plasticity,
652 morphological variation and evolvability: a multilevel analysis of morphometric
653 integration in the shape of compound leaves. J. Evol.Biol. 25:115–129 (2012).
654 51. Figueirido B, Tseng ZJ, Martín-Serra A: Skull shape evolution in durophagous
655 carnivorans. Evolution 67, 1975-1993 (2013).
656 52. Klingenberg C.P. & Marugán-Lobón, J. Evolutionary covariation in geometric
657 morphometric data: analyzing integration, modularity, and allometry in a phylogenetic
658 context. Syst Biol 62:591-610 (2013).
659 53. Martin-Serra A., Figueirido B. & Palmqvist P. A three-dimensional analysis of the
660 morphological evolution and locomotor behaviour of the carnivoran hind limb. BMC
661 Evol. Biol. 14:129 (2014).
662 54. Martin-Serra A, Figueirido B, Perez-Claros, J.A. & Palmqvist P. 2015. Patterns of
663 morphological integration in the appendicular skeleton of mammalian carnivores
664 Evolution 69: 321–340.
665 55. Monteiro, L. R. Multivariate regression models and geometric morphometrics: the
666 search for causal factors in the analysis of shape. Syst. Biol. 48, 192-199 (1999).
667 56. Felsenstein, J. J. Phylogenies and the comparative method. Am. Nat. 125, 1-15
668 (1985).
669 57. Drake, A. G. & Klingenberg, C. P. The pace of morphological change: historical
670 transformation of skull shape in St Bernard dogs. Proc. R. Soc. London Ser. B 275, 71-
671 56 (2008).
672 58. Midford, P. E., Garland Jr, T., & Maddison, W. P. PDAP package of Mesquite,
673 version 1.14. Available via http://mesquiteproject. org/pdap_mesquite (2008).

674 59. Ewer, R. F. The Carnivores. (Cornell Univ. Press, Ithaca, NY, 1973).
675 60. Figueirido, B., Pérez-Claros, J. A., Torregrosa, V., Martín-Serra, A., & Palmqvist, P.
676 Demythologizing Arctodus simus, the 'short-faced'long-legged and predaceous bear
677 that never was. J. Vertebr. Paleontol. 30, 262-275 (2010).
678 61. Mitteroecker, P., & Bookstein, F. Linear discrimination, ordination, and the
679 visualization of selection gradients in modern morphometrics. Evol. Biol. 38, 100-114
680 (2011).
681 62. Harmon, L. J., Weir, J. T., Brock, C. D., Glor, R. E., & Challenger, W. GEIGER:
682 investigating evolutionary radiations. Bioinformatics 24, 129-131 (2008).
683 63. Carbone, C., Mace, G. M., Roberts, S. C. & Macdonald, D. W. Energetic constraints
684 on the diet of terrestrial carnivores. Nature 402, 286-288 (1999).
685 64. Andersson, K. Predicting carnivoran body mass from a weight-bearing joint. J. Zool.
686 Lond. 262, 161-172 (2004).
687 65. Torregrosa, V., Petrucci, M., Pérez-Claros, J. A., & Palmqvist, P. Nasal aperture area
688 and body mass in felids: Ecophysiological implications and paleobiological inferences.
689 Geobios 43, 653-661 (2010).
690 66. Figueirido, B., Pérez-Claros, J.A., Hunt, R.M. Jr., & Palmqvist, P. Body mass
691 estimation in amphicyonid carnivoran mammals: A multiple regression approach from
692 the skull and skeleton. Acta Palaeontol. Pol. 56, 225-246 (2011).
693 67. Van Valkenburgh, B. in Body Size in Mammalian Paleobiology (eds Damuth, J. &
694 MacFadden, B. M.) 1-11 (Cambridge Univ. Press, 1990).
695 68. Lucas, P., Constantino, P., Wood, B., & Lawn, B. Dental enamel as a dietary
696 indicator in mammals. BioEssays 30, 374-385 (2008).

69. Tseng, Z. J. Variation and implications of intra-dentition Hunter-Schreger band pattern in fossil hyaenids and canids (Carnivora, Mammalia). J. Vertebr. Paleontol. 31, 1163-1167 (2011).

70. Stefen, C. [Zahnschmelzdifferenzierungen bei Raubtieren: Carnivora im Vergleich zu Vertretern der Creodonta, Arctocyonidae, Mesonuchidae, Entelodontidae (Placentalia), Thylacoleonidae, Dasyuridae und Thylaacinidae (Marsupialia)], Bonn, , Germany, 189 pp. [German]: Rheinischen Friedrich-Wilhelms-Universtat zu Bonn. Ph.D. dissertation (1994).

**ACKNOWLEDGEMENTS**

We thank to J. Galkin, E. Westwig and Judy Chupasko for assistance. We also thank David Polly and Blaire Van Valkenburgh for their comments on an earlier version of this manuscript. Funding for this project was provided by the "Spanish Ministry of Economy and Competitiveness (MINNECO)" (CGL2012-37866) to B.F, a Bushnell Foundation Grant (Brown University) to C.M.J., and NSF DEB-1257572 and Frick Postdoctoral Fellowship (American Museum of Natural History) to ZJT.

**AUTHOR CONTRIBUTION**

B.F., C.M.J., Z.J.T. and A.M.S. designed the study. B.F., C.M.J. and Z.J.T. performed data entry, analytical work and wrote the paper; A.M.S performed analytical work and assisted with figures. C.M.J. assisted with writing and figures.

Competing financial interests: The authors declare no competing financial interests.

**FIGURE LEGENDS**

**Figure 1**. The elbow-joint structure. **a**, anatomy of the elbow-joint exemplified in a 3D model of *Panthera onca* (jaguar) showing the six 2D-*landmarks* digitized (circles) to capture the shape of the anterior surface of the humerus distal epiphysis (elbow-joint) of living predators and extinct canids. **b**, elbow-joint shape differences between the three present-day predatory groups. From up to down: *Panthera tigris* (ambush predator), *Vulpes vulpes* (Pounce-pursuit predators) and, *Lycaon pictus* (pursuit predator). Abbreviations: fe, entepicondylar foramen.

**Figure 2.** Canonical Variates Analysis. **a**, contour plot depicted from the functions obtained in CVA performed from the elbow shape of living predators and the predatory grouping. **b**, elbow shape variation accounted for by the first canonical function (up) and for by the second canonical function (bottom). Black arrows denote shape changes. **c**, contour plot depicted from the functions obtained in CVA performed from the elbow shape of living predators and the predatory grouping, but now including fossil forms. Number indicates species: 1, *Hesperocyon gregarius*; 2, *Osbornodon fricki*; 3, *Mesocyon temnodon*; 4, *Enhydrocyon crassidens*; 5, *Mesocyon coryphaeus*; 6, *Archeocyon leptodus*; 7, *Archeocyon falkenbachi*; 8, *Phlaocyon leucososteus*; 9, *Cormocyon hyaedeni*; 10, *Desmocyon thomsoni*; 11, *Cynarctus crucidens*; 12, *Psalidocyon marianae*; 13, *Epicyon saevus*; 14, *Epicyon haydeni*; 15, *Borophagus pugantor*; 16*, Borophagus parvus*; 17, *Borophagus secundus*; 18, *Carpocyon webbi*; 19, *Aelurodon asthenostylus*; 20, *Aelurodon mcgrewi*; 21, *Aelurodon taxoides*; 22*, Aelurodon ferox*; 23, *Leptocyon vulpinus*; 24, *Leptocyon vafer*; 25, *Leptocyon matthewi*; 26, *Vulpes stenognathus*; 27, *Urocyon minicephalus*; 28, *Eucyon davisi*; 29, *Canis thooides*; 30, *Canis armbrusteri*; 31, *Canis dirus*; 32, *Canis lupus*.

**Figure 3**. Reconstruction of elbow-shape ancestral states. **a**, phylogeny of canids showing their temporal ranges (colours are the average scores obtained in CVA for each

747 species. **b**, representation of ancestral elbow shapes using squared-changed
748 parsimony[26]. Nodes 13, 18, 34 are the basal nodes for the three subfamilies, Node 35 is
749 the basal for the tribe Canini plus Vulpini and, Node 37 is the basal for the tribe Canini
750 typical of pursuit predators. Black arrows indicate morphological changes.

751 **Figure 4.** Elbow-joint shape evolution in canids related to environmental change. **a**,
752 major vegetational transitions trough the Cenozoic of North America[11] and major
753 environmental events[12,24], respectively. The light-grey box indicates the proposed timing
754 for the spread of open-habitat grasses (23-27Ma)[12] and the dark-grey box represent the
755 shift in plant communities from $C_3$ to $C_4$ grasses (5-8 Ma)[24]. The black dot represent the
756 Middle Miocene Climatic Optimum (MMECO) at 16 Ma[35]. b, three-dimensional
757 morphospaces at different time intervals showing the relationship of elbow shape and
758 the enamel layer arrangement (HSB) in extinct canids, as proxy for habitat openness.
759 Each graph represents the mean of enamel data of those taxa present in different time
760 intervals superimposed to their corresponding position in Figure 2c. Numbers denotes
761 species: 5, *Mesocyon coryphaeus*; 8, *Phlaocyon leucososteus*; 10, *Desmocyon thomsoni*;
762 11, *Cynarctus crucidens*; 13, *Epicyon saevus*; 14, *Epicyon haydeni*; 16*, Borophagus*
763 *parvus*; 17, *Borophagus secundus*; 18, *Carpocyon webbi*; 19, *Aelurodon asthenostylus*;
764 21, *Aelurodon taxoides*; 22*, Aelurodon ferox*; 30, *Canis armbrusteri*; 31, *Canis dirus*;
765 32, *Canis lupus*.

766

767 **TABLES**

768 **Table 1.** Sample size of extant carnivorans used in this study. Each species was
769 classified into one of the three present-day predatory groups following Ref. 23 with the
770 sole exception of the cheetah (*Acynonix jubatus*).

771

| SPECIES | COMMON NAME | MUSEUM Nº | FAMILY | GROUP |
|---|---|---|---|---|
| ***Acinonyx jubatus*** | cheetah | AMNH-119656 | FELIDAE | Pursuit |
| ***Acinonyx jubatus*** | cheetah | AMNH-119682 | FELIDAE | Pursuit |
| ***Acinonyx jubatus*** | cheetah | AMNH-119655 | FELIDAE | Pursuit |
| ***Acinonyx jubatus*** | cheetah | AMNH-35307 | FELIDAE | Pursuit |
| ***Acinonyx jubatus*** | cheetah | AMNH-80172 | FELIDAE | Pursuit |
| ***Canis adustus*** | side-striped jackal | AMNH-14174 | CANIDAE | Pounce |
| ***Canis adustus*** | side-striped jackal | AMNH-216334 | CANIDAE | Pounce |
| ***Canis adustus*** | side-striped jackal | AMNH-33322 | CANIDAE | Pounce |
| ***Canis adustus*** | side-striped jackal | AMNH-52049 | CANIDAE | Pounce |
| ***Canis adustus*** | side-striped jackal | AMNH-80662 | CANIDAE | Pounce |
| ***Canis aureus*** | golden jackal | AMNH-1877144 | CANIDAE | Pounce |
| ***Canis aureus*** | golden jackal | AMNH-27741 | CANIDAE | Pounce |
| ***Canis aureus*** | golden jackal | AMNH-54516 | CANIDAE | Pounce |
| ***Canis latrans*** | coyote | AMNH-123036 | CANIDAE | Pounce |
| ***Canis latrans*** | coyote | AMNH-131833 | CANIDAE | Pounce |
| ***Canis latrans*** | coyote | AMNH-136419 | CANIDAE | Pounce |
| ***Canis latrans*** | coyote | AMNH-141153 | CANIDAE | Pounce |
| ***Canis latrans*** | coyote | AMNH-99653 | CANIDAE | Pounce |
| ***Canis lupus*** | wolf | AMNH-134940 | CANIDAE | Pursuit |
| ***Canis lupus*** | wolf | AMNH-244144 | CANIDAE | Pursuit |
| ***Canis lupus*** | wolf | AMNH-98225 | CANIDAE | Pursuit |
| ***Canis lupus*** | wolf | AMNH-98226 | CANIDAE | Pursuit |
| ***Canis lupus*** | wolf | AMNH-98230 | CANIDAE | Pursuit |
| ***Canis mesomelas*** | black-backed jackal | AMNH-187711 | CANIDAE | Pounce |
| ***Canis mesomelas*** | black-backed jackal | AMNH-114228 | CANIDAE | Pounce |
| ***Canis mesomelas*** | black-backed jackal | AMNH-34731 | CANIDAE | Pounce |
| ***Canis mesomelas*** | black-backed jackal | AMNH-34732 | CANIDAE | Pounce |
| ***Canis mesomelas*** | black-backed jackal | AMNH-54209 | CANIDAE | Pounce |
| ***Canis simensis*** | Ethiopian wolf | AMNH-214799 | CANIDAE | Pounce |
| ***Civettictis civetta*** | African civet | MCZ-37920 | VIVERRIDAE | Pounce |
| ***Crocuta crocuta*** | spotted hyena | AMNH-187781 | HYAENIDAE | Pursuit |
| ***Crocuta crocuta*** | spotted hyena | AMNH-114227 | HYAENIDAE | Pursuit |
| ***Crocuta crocuta*** | spotted hyena | AMNH-27765 | HYAENIDAE | Pursuit |
| ***Crocuta crocuta*** | spotted hyena | AMNH-27767 | HYAENIDAE | Pursuit |
| ***Crocuta crocuta*** | spotted hyena | AMNH-52097 | HYAENIDAE | Pursuit |
| ***Cuon alpinus*** | dhole | AMNH-54842 | CANIDAE | Pursuit |
| ***Cuon alpinus*** | dhole | AMNH-54976 | CANIDAE | Pursuit |
| ***Felis caracal*** | desert lynx | AMNH-113794 | FELIDAE | Ambush |
| ***Felis caracal*** | desert lynx | AMNH-90105 | FELIDAE | Ambush |
| ***Felis caracal*** | desert lynx | AMNH-187788 | FELIDAE | Ambush |
| ***Felis silvestris*** | cat | AMNH-244096 | FELIDAE | Ambush |
| ***Gulo gulo*** | wolverine | AMNH-52977 | MUSTELIDAE | Ambush |
| ***Gulo gulo*** | wolverine | MCZ-48566 | MUSTELIDAE | Ambush |
| ***Gulo gulo*** | wolverine | MCZ-5131 | MUSTELIDAE | Ambush |
| ***Hyaena hyaena*** | striped hyena | AMNH-05 | HYAENIDAE | Pounce |
| ***Hyaena hyaena*** | striped hyena | AMNH-24436 | HYAENIDAE | Pounce |
| ***Hyaena hyaena*** | striped hyena | AMNH-54431 | HYAENIDAE | Pounce |
| ***Hyaena hyaena*** | striped hyena | AMNH-54512 | HYAENIDAE | Pounce |

| | | | | |
|---|---|---|---|---|
| ***Lycaon pictus*** | African wild dog | AMNH-82085 | CANIDAE | Pursuit |
| ***Lycaon pictus*** | African wild dog | AMNH-82086 | CANIDAE | Pursuit |
| ***Lycaon pictus*** | African wild dog | AMNH-82087 | CANIDAE | Pursuit |
| ***Lycaon pictus*** | African wild dog | AMNH-82088 | CANIDAE | Pursuit |
| ***Lycaon pictus*** | African wild dog | AMNH-85154 | CANIDAE | Pursuit |
| ***Lynx pardina*** | European lynx | AMNH-169492 | FELIDAE | Ambush |
| ***Panthera leo*** | lion | AMNH-54995 | FELIDAE | Ambush |
| ***Panthera leo*** | lion | AMNH- | FELIDAE | Ambush |
| ***Panthera leo*** | lion | AMNH-54996 | FELIDAE | Ambush |
| ***Panthera leo*** | lion | AMNH- | FELIDAE | Ambush |
| ***Panthera onca*** | jaguar | AMNH-135928 | FELIDAE | Ambush |
| ***Panthera onca*** | jaguar | AMNH-135929 | FELIDAE | Ambush |
| ***Panthera onca*** | jaguar | AMNH-139959 | FELIDAE | Ambush |
| ***Panthera pardus*** | leopard | AMNH- | FELIDAE | Ambush |
| ***Panthera pardus*** | leopard | AMNH-34475 | FELIDAE | Ambush |
| ***Panthera tigris*** | tiger | AMNH-100024 | FELIDAE | Ambush |
| ***Panthera tigris*** | tiger | AMNH-113743 | FELIDAE | Ambush |
| ***Panthera tigris*** | tiger | AMNH-113744 | FELIDAE | Ambush |
| ***Panthera tigris*** | tiger | AMNH-113748 | FELIDAE | Ambush |
| ***Panthera tigris*** | tiger | AMNH-135846 | FELIDAE | Ambush |
| ***Panthera tigris*** | tiger | AMNH-54605 | FELIDAE | Ambush |
| ***Panthera tigris*** | tiger | AMNH-135847 | FELIDAE | Ambush |
| ***Panthera uncia*** | snow leopard | AMNH-100110 | FELIDAE | Ambush |
| ***Panthera uncia*** | snow leopard | AMNH-166952 | FELIDAE | Ambush |
| ***Panthera uncia*** | snow leopard | AMNH-207704 | FELIDAE | Ambush |
| ***Panthera uncia*** | snow leopard | AMNH-35476 | FELIDAE | Ambush |
| ***Puma concolor*** | puma | AMNH-183357 | FELIDAE | Ambush |
| ***Puma concolor*** | puma | AMNH-244616 | FELIDAE | Ambush |
| ***Puma concolor*** | puma | AMNH-80451 | FELIDAE | Ambush |
| ***Puma concolor*** | puma | AMNH-87803 | FELIDAE | Ambush |
| ***Speothos venaticus*** | bush dog | MCZ-28056 | CANIDAE | Pounce |
| ***Speothos venaticus*** | bush dog | NHM-1966.1.24.1 | CANDIAE | Pounce |
| ***Urocyon cinereoargenteus*** | gray fox | AMNH-147213 | CANIDAE | Pounce |
| ***Urocyon cinereoargenteus*** | gray fox | AMNH-208379 | CANIDAE | Pounce |
| ***Urocyon cinereoargenteus*** | gray fox | AMNH-35595 | CANIDAE | Pounce |
| ***Urocyon cinereoargenteus*** | gray fox | AMNH-35682 | CANIDAE | Pounce |
| ***Viverra zibetha*** | large indian civet | MCZ-35916 | VIVERIDAE | Pounce |
| ***Vulpes macrotis*** | kit fox | AMNH-131834 | CANIDAE | Pounce |
| ***Vulpes velox*** | swift fox | AMNH-100190 | CANIDAE | Pounce |
| ***Vulpes velox*** | swift fox | AMNH-100215 | CANIDAE | Pounce |
| ***Vulpes vulpes*** | red fox | AMNH-128486 | CANIDAE | Pounce |
| ***Vulpes vulpes*** | red fox | AMNH-128488 | CANIDAE | Pounce |
| ***Vulpes vulpes*** | red fox | AMNH-128490 | CANIDAE | Pounce |
| ***Vulpes vulpes*** | red fox | AMNH-166938 | CANIDAE | Pounce |
| ***Vulpes vulpes*** | red fox | AMNH-98163 | CANIDAE | Pounce |

772

773

774

**Table 2.** Results of the Canonical Variates Analysis. Mahalanobis distances (in bold) plus Procrustes distances and the associated *P*-values obtained from the permutations (10,000 rounds) computed among all possible pairs of groups of extant predators are shown. Sample size: Pursuit predators (N = 22); Pounce predators (N = 38); Ambush predators (N = 32).

| | PURSUIT | POUNCE |
|---|---|---|
| POUNCE | **2.1216 (*P*<.0001)**<br>0.0551 (*P*<.0065) | ----- |
| AMBUSH | **3.6614 (*P*<.0001)**<br>0.1281 (*P*<.0001) | **3.9774 (*P*<.0001)**<br>0.1504 (*P*<.0001) |

**Table 3.** Fossil data, museum numbers, geographical localities, and the subfamilies to which specimens belong as well as their stratigraphic ranges were taken from Ref. 17 for the Hesperocyoninae, from Ref. 18 for the Borophaginae and from Ref. 19 for the Caninae. FAD: First appearance of taxa; LAD: last appearance of taxa; MP: midpoint. FAD, LAD and MP are given in million years before present.

| FOSSIL SPECIMENS | # | MUSEUM Nº | GEOGRAPHIC LOCATION | SUBFAMILY | LAD (Ma) | FA (M |
|---|---|---|---|---|---|---|
| ***Aelurodon asthenostylus*** | 19 | F:AM-28356 | Colorado | BOROPHAGINAE | 14 | |
| ***Aelurodon ferox*** | 22 | AMNH-61723 | New Mexico | BOROPHAGINAE | 12 | |
| ***Aelurodon ferox*** | 22 | AMNH-70624 | Nebraska | BOROPHAGINAE | 12 | |

| | | | | | | |
|---|---|---|---|---|---|---|
| ***Aelurodon mcgrewi*** | 20 | AMNH-22410 | Nebraska | BOROPHAGINAE | 13 | |
| ***Aelurodon taxoides*** | 21 | AMNH-30902 | Kansas | BOROPHAGINAE | 9 | |
| ***Aelurodon taxoides*** | 21 | F:AM-67481 | South Dakota | BOROPHAGINAE | 9 | |
| ***Archeocyon falkenbachi*** | 7 | F:AM-49029 | Wyoming | BOROPHAGINAE | 24 | |
| ***Archeocyon leptodus*** | 6 | F:AM-49060 | Wyoming | BOROPHAGINAE | 24 | |
| ***Borophagus parvus*** | 16 | F:AM-67955 | Arizona | BOROPHAGINAE | 5 | |
| ***Borophagus pugantor*** | 15 | F:AM-67838 | Colorado | BOROPHAGINAE | 5 | |
| ***Borophagus secundus*** | 17 | F:AM-67647 | Kansas | BOROPHAGINAE | 5 | |
| ***Borophagus secundus*** | 17 | F:AM-67650 | Kansas | BOROPHAGINAE | 5 | |
| ***Canis armbrusteri*** | 30 | F:AM-95181 | Kansas | CANINAE | 0.2 | |
| ***Canis armbrusteri*** | 30 | AMNH-96633 | Arkansas | CANINAE | 0.2 | |
| ***Canis armbrusteri*** | 30 | F:AM-68017 | Florida | CANINAE | 0.2 | |
| ***Canis dirus*** | 31 | F:AM-97078 | No data | CANINAE | 0.05 | 0. |
| ***Canis dirus*** | 31 | F:AM-67302 | México | CANINAE | 0.05 | 0. |
| ***Canis sp. (cf lupus)*** | 32 | F:AM-30444 | Alaska | CANINAE | 0 | |
| ***Canis sp. (cf lupus)*** | 32 | F:AM-68006 | Alaska | CANINAE | 0 | |
| ***Canis lupus*** | 32 | F:AM-8582 | Oregon | CANINAE | 0 | |
| ***Canis sp.*** | 32 | F:AM-1937(1064) | No locality data | CANINAE | 0 | |
| ***Canis thooides*** | 29 | F:AM-63101 | Arizona | CANINAE | 1.7 | 2 |
| ***Carpocyon webbi*** | 18 | F:AM-27366E | New Mexico | BOROPHAGINAE | 10 | |
| ***Cormocyon hyaedeni*** | 9 | F:AM-49448 | South Dakota | BOROPHAGINAE | 19 | |
| ***Cynarctus crucidens*** | 11 | F:AM-49172 | Nebraska | BOROPHAGINAE | 9 | |
| ***Desmocyon thomsoni*** | 10 | AMNH-49017 | Wyoming | BOROPHAGINAE | 17.5 | |
| ***Enhydrocyon crassidens*** | 5 | AMNH-12886 | South Dakota | HESPEROCYONINAE | 21 | |
| ***Epicyon haydeni*** | 14 | F:AM-67403E | Nebraska | BOROPHAGINAE | 5 | |
| ***Epicyon haydeni*** | 14 | F:AM-67602 | Kansas | BOROPHAGINAE | 5 | |
| ***Epicyon haydeni*** | 14 | F:AM-67826 | Colorado | BOROPHAGINAE | 5 | |
| ***Epicyon saevus*** | 13 | F:AM-67489 | South Dakota | BOROPHAGINAE | 5 | |
| ***Eucyon davisi*** | 28 | F:AM-72555 | Arizona | CANINAE | 5 | |
| ***Eucyon davisi*** | 28 | F:AM-72557 | Arizona | CANINAE | 5 | |
| ***Eucyon davisi*** | 28 | F:AM 72559 | Arizona | CANINAE | 5 | |
| ***Hesperocyon gregarius*** | 1 | F:AM-63357 | South Dakota | HESPEROCYONINAE | 29 | |
| ***Leptocyon vulpinus*** | 25 | AMNH-12883 | South Dakota | CANINAE | 18 | |
| ***Leptocyon matthewi*** | 24 | F:AM-72707 | Nebraska | CANINAE | 9 | 12 |
| ***Leptocyon vafer*** | 24 | F:AM-72701 | Nebraska | CANINAE | 9 | |
| ***Leptocyon vafer*** | 23 | F:AM-72701C | Nebraska | CANINAE | 9 | |
| ***Mesocyon coryphaeus*** | 4 | AMNH-6920 | Oregon | HESPEROCYONINAE | 21 | |
| ***Mesocyon temnodon*** | 3 | F:AM-102381 | Wyoming | HESPEROCYONINAE | 25 | |
| ***Osbornodon fricki*** | 2 | F:AM-27363 | New Mexico | HESPEROCYONINAE | 15 | |
| ***Phlaocyon leucososteus*** | 8 | AMNH-8768 | Colorado | BOROPHAGINAE | 16 | |
| ***Psalidocyon marianae*** | 12 | AMNH-27397 | New Mexico | BOROPHAGINAE | 15 | |
| ***Urocyon minicephalus*** | 27 | AMNH-68024A | Florida | CANINAE | 0.4 | |
| ***Urocyon minicephalus**** | 27 | AMNH-67295 | Florida | CANINAE | 0.4 | |
| ***Vulpes stenognathus*** | 26 | F:AM-62990 | Arizona | CANINAE | 5 | |

807

808

809

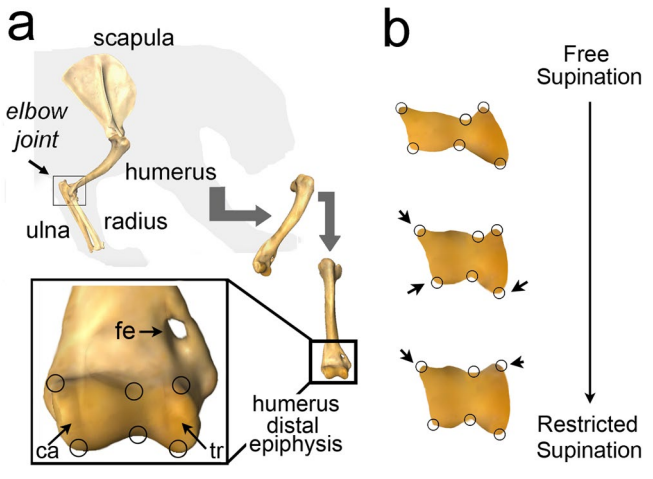
a
scapula
elbow joint
humerus
ulna
radius
fe
ca
tr
humerus distal epiphysis
b
Free Supination
Restricted Supination

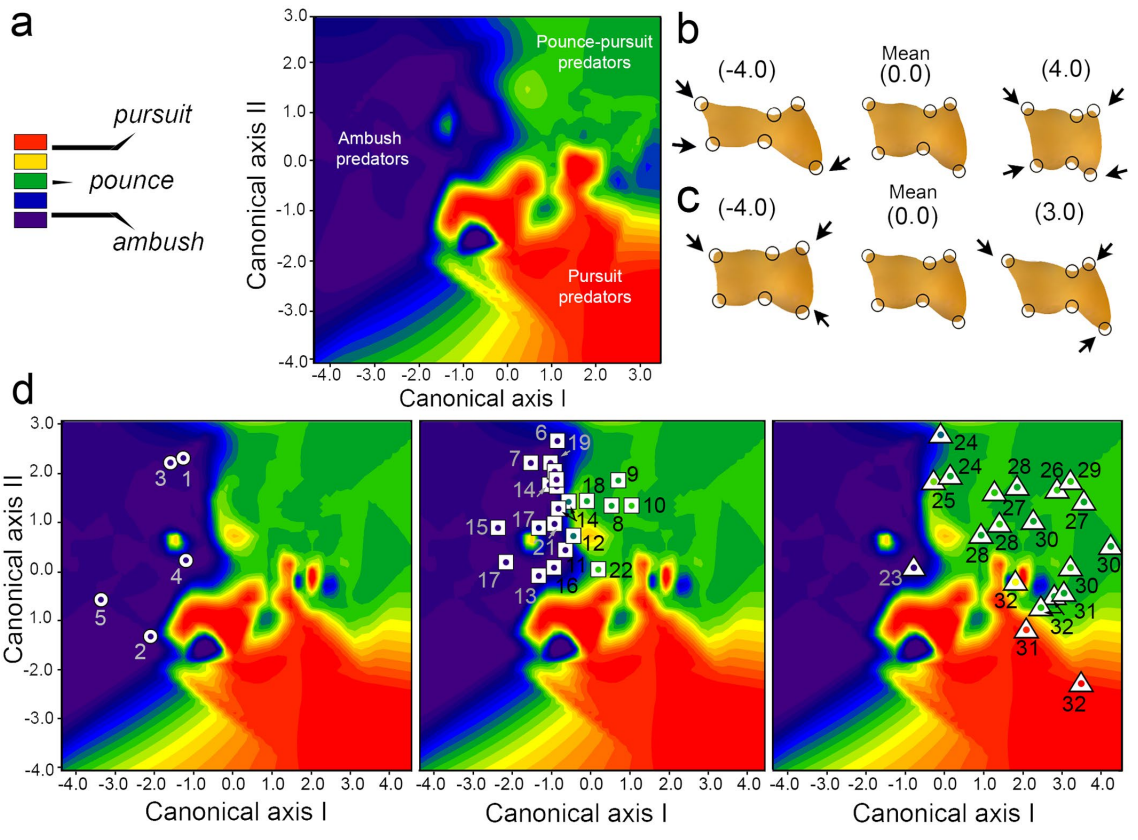
a
pursuit
pounce
ambush
Pounce-pursuit predators
Ambush predators
Pursuit predators
Canonical axis II
Canonical axis I
b
(-4.0)
Mean (0.0)
(4.0)
c
(-4.0)
Mean (0.0)
(3.0)
d
Canonical axis II
Canonical axis I
Canonical axis I
Canonical axis I

817

818

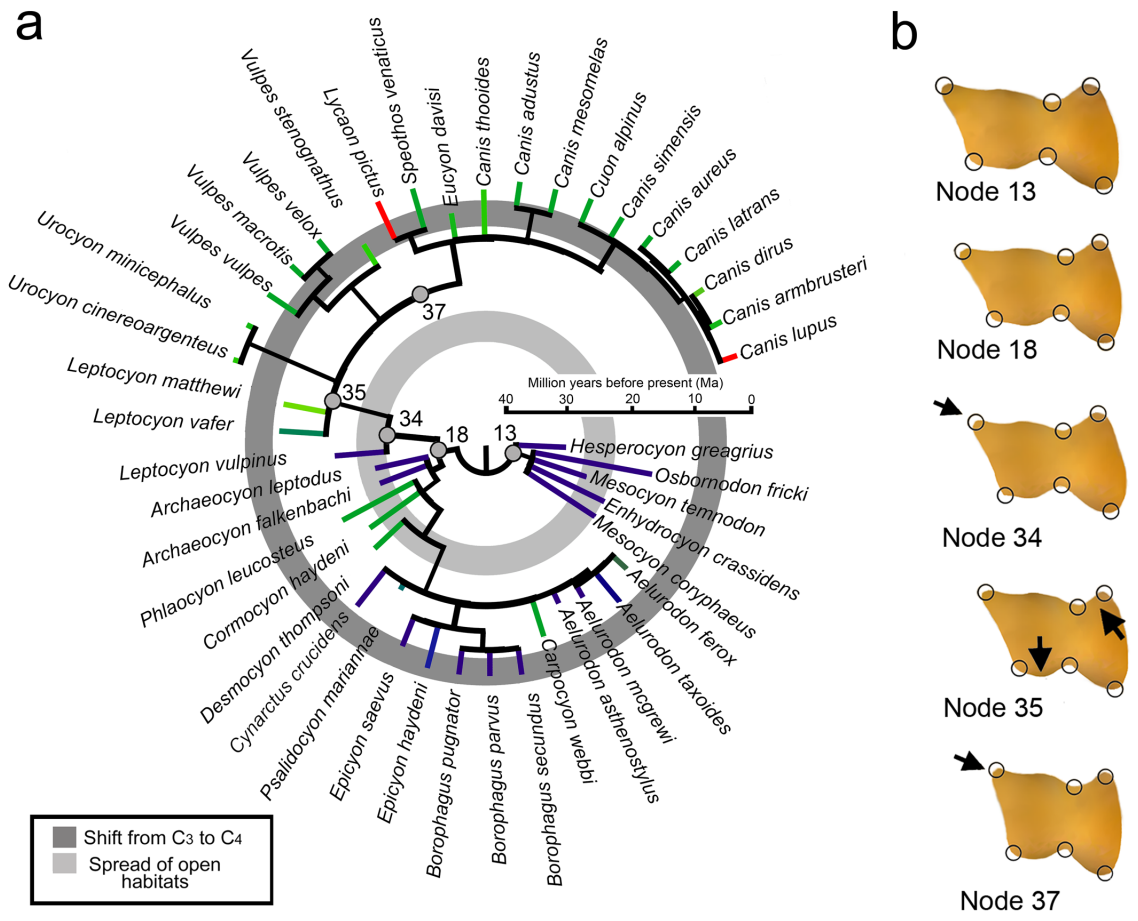
a
b
Vulpes stenognathus
Lycaon pictus
Speothos venaticus
Eucyon davisi
Canis thooides
Canis adustus
Canis mesomelas
Cuon alpinus
Canis simensis
Canis aureus
Canis latrans
Canis dirus
Canis armbrusteri
Canis lupus
Vulpes velox
Vulpes macrotis
Vulpes vulpes
Urocyon minicephalus
Urocyon cinereoargenteus
Leptocyon matthewi
Leptocyon vafer
Leptocyon vulpinus
Archaeocyon leptodus
Archaeocyon falkenbachi
Phlaocyon leucosteus
Cormocyon haydeni
Desmocyon thompsoni
Cynarctus crucidens
Psalidocyon marianae
Epicyon saevus
Epicyon haydeni
Borophagus pugnator
Borophagus parvus
Borophagus secundus
Carpocyon webbi
Aelurodon asthenostylus
Aelurodon mcgrewi
Aelurodon taxoides
Aelurodon ferox
Mesocyon coryphaeus
Mesocyon crassidens
Enhydrocyon temnodon
Osbornodon fricki
Hesperocyon greagrius
37
35
34
18
13
Million years before present (Ma)
40
30
20
10
0
Shift from C3 to C4
Spread of open habitats
Node 13
Node 18
Node 34
Node 35
Node 37

819

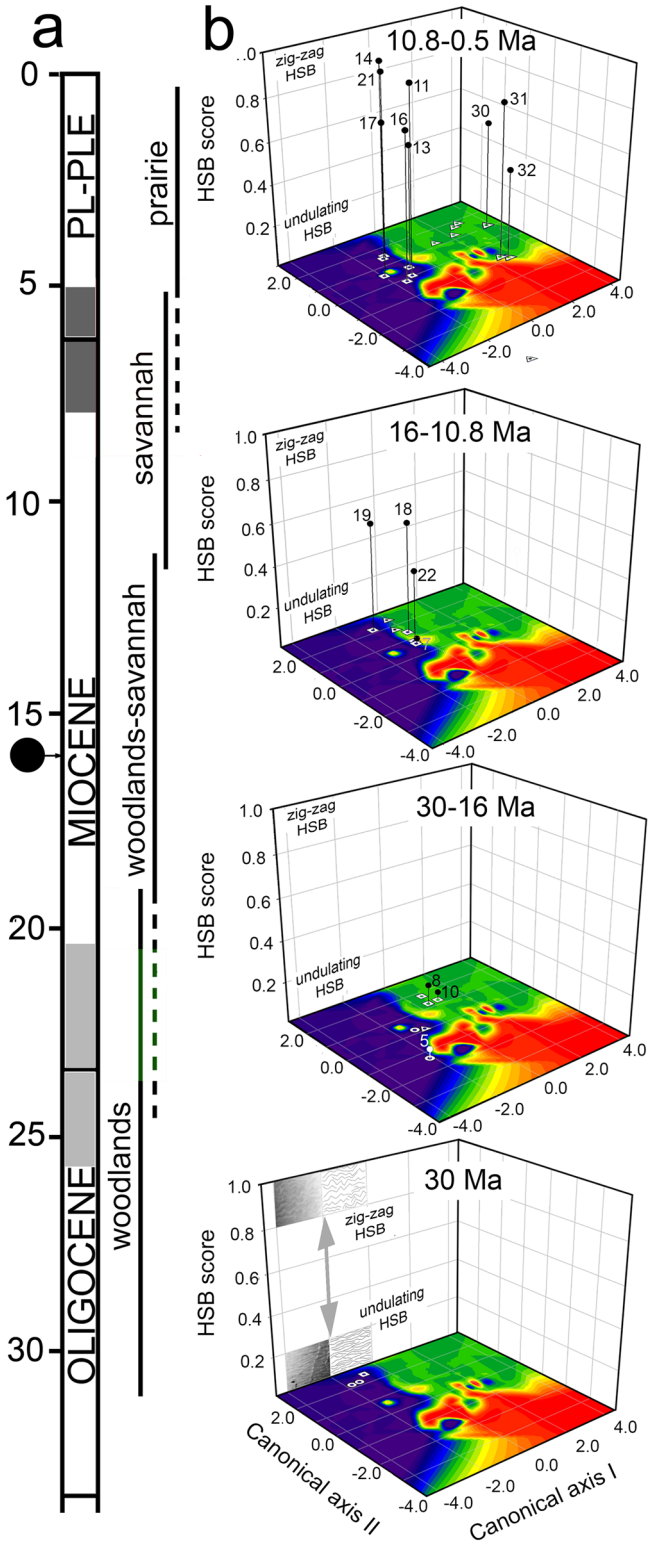
a
b
0
5
10
15
20
25
30
PL-PLE
MIOCENE
OLIGOCENE
prairie
savannah
woodlands-savannah
woodlands
10.8-0.5 Ma
16-10.8 Ma
30-16 Ma
30 Ma
zig-zag HSB
undulating HSB
HSB score
Canonical axis I
Canonical axis II

820